

Non-MHV Tree Amplitudes in Gauge Theory

George Georgiou, E. W. N. Glover and Valentin V. Khoze

*Institute of Particle Physics Phenomenology, Department of Physics,
University of Durham, Durham, DH1 3LE, UK*

E-mail: george.georgiou, e.w.n.glover, valya.khoze@durham.ac.uk

ABSTRACT: We show how all non-MHV tree-level amplitudes in $0 \leq \mathcal{N} \leq 4$ gauge theories can be obtained directly from the known MHV amplitudes using the scalar graph approach of Cachazo, Svrcek and Witten. Generic amplitudes are given by sums of inequivalent scalar diagrams with MHV vertices. The novel feature of our method is that after the ‘Feynman rules’ for scalar diagrams are used, together with a particular choice of the reference spinor, no further helicity-spinor algebra is required to convert the results into a numerically usable form. Expressions for all relevant individual diagrams are free of singularities at generic phase space points, and amplitudes are manifestly Lorentz- (and gauge-) invariant. To illustrate the method, we derive expressions for n -point amplitudes with three negative helicities carried by fermions and/or gluons. We also write down a supersymmetric expression based on Nair’s supervertex which gives rise to all such amplitudes in $0 \leq \mathcal{N} \leq 4$ gauge theories.

1. Introduction

In a recent paper Cachazo, Svrcek and Witten [1] proposed a remarkable new approach for calculating tree-level scattering amplitudes of n gluons. In this approach tree amplitudes in gauge theory are found by summing tree-level scalar diagrams. The CSW formalism [1] is constructed in terms of scalar propagators, $1/q^2$, and tree-level maximal helicity violating (MHV) amplitudes, which are interpreted as new scalar vertices. This novel diagrammatic approach follows from an earlier construction of Witten [2] which related perturbative amplitudes of conformal $\mathcal{N} = 4$ supersymmetric gauge theory to D-instanton contributions in a topological string theory in twistor space.

The results of [2, 1] have been tested and further developed in gauge theory in [3, 4, 5, 6, 7], and in string theory and supergravity in [8, 9, 10, 11, 12, 13, 14, 15, 16].

In [3] the CSW diagrammatic approach [1] was extended to gauge theories with fermions, and it was also shown that supersymmetry is not required for the construction to work. At tree level the scalar graph formalism works in supersymmetric and non-supersymmetric theories, including QCD.

The motivation of the present paper is to show how non-MHV (NMHV) tree-level amplitudes in $0 \leq \mathcal{N} \leq 4$ gauge theories can be obtained directly from the scalar graph approach. One of the main points we want to make is that after the ‘Feynman rules’ for scalar diagrams are used, together with the off-shell continuation of helicity spinors on internal lines, expressions for all relevant individual diagrams are automatically free of unphysical singularities at generic phase space points, and amplitudes are manifestly Lorentz- (and gauge-) invariant. Hence, no further helicity-spinor algebra is required to convert the results into an immediately usable form.

To illustrate the method, we will derive expressions for n -point amplitudes with three negative helicities carried by fermions and/or gluons. We will also write down a supersymmetric expression which gives rise to all such amplitudes in $0 \leq \mathcal{N} \leq 4$ gauge theories. This compliments a very recent calculation of Kosower [6] of such amplitudes in the purely gluonic case.

As in [3], we will consider tree-level amplitudes in a generic $SU(N)$ gauge theory with an arbitrary finite number of colours. $SU(N)$ is unbroken and all fields are taken to be massless, we refer to them generically as gluons, fermions and scalars. The gauge theory is not necessarily

assumed to be supersymmetric, i.e. the number of supercharges is $4\mathcal{N}$, where $0 \leq \mathcal{N} \leq 4$.

This paper is organised as follows. In section 2 we will use supersymmetric Ward identities to express NMHV purely gluonic amplitudes in terms of NMHV amplitudes with gluons and two fermions¹. Then, using the CSW scalar graph method for gluons [1] and fermions [3], in sections 3 and 4 we will derive expressions for the NMHV amplitudes with three negative helicities involving gluons and fermions.

Section 5 of this paper considers the scalar graph method with the single analytic supervertex of Nair [17]. We provide a single formula which gives rise to all tree-level NMHV amplitudes with three negative helicities in $0 \leq \mathcal{N} \leq 4$ supersymmetric gauge theories, involving all possible configurations of gauge fields, fermions and scalars. There is also no principle obstacle to continue with further iterations of the analytic supervertex and derive formal expressions for tree amplitudes with an arbitrary number of negative helicities. Depending on the topology of the iteration, these expressions would correspond to different skeleton diagrams of [5] in $0 \leq \mathcal{N} \leq 4$ supersymmetric gauge theories.

We end the introduction with a brief review of the spinor helicity formalism and definitions of the MHV amplitudes.

1.1 Amplitudes in the spinor helicity formalism

Using colour decomposition, an n -point amplitude \mathcal{M}_n can be represented as a sum of products of colour factors T_n and purely kinematic partial amplitudes A_n . The latter have the colour information stripped off and hence do not distinguish between fundamental quarks and adjoint gluinos. The scalar graph method [1] is used to evaluate only the purely kinematic amplitudes A_n . Full amplitudes are then determined uniquely from the kinematic part A_n , and the known expressions for T_n .

We will first consider theories with $\mathcal{N} \leq 1$ supersymmetry. Gauge theories with extended supersymmetry have a more intricate behaviour of their amplitudes in the helicity basis and their study will be postponed until section 5. Theories with $\mathcal{N} = 4$ (or $\mathcal{N} = 2$) supersymmetry have \mathcal{N} different species of gluinos and 6 (or 4) scalar fields. This leads to a large number of elementary MHV-like vertices in the scalar graph formalism. This proliferation of elementary

¹It may be worthwhile to note that while a gluonic non-MHV amplitude can be determined in terms of amplitudes with fermions and gluons, the converse of this statement is not true. Individual non-MHV amplitudes involving fermions cannot be deduced with susy Ward identities from amplitudes with gluons only.

vertices asks for a super-graph generalization of the CSW scalar graph method, which will be outlined in section 5.

Now we concentrate on tree level partial amplitudes $A_n = A_{l+2m}$ with l gluons and $2m$ fermions in the helicity basis, and all external lines are defined to be incoming.

In $\mathcal{N} \leq 1$ theory a fermion of helicity $+\frac{1}{2}$ is always connected by a fermion propagator to a helicity $-\frac{1}{2}$ fermion hence the number of fermions $2m$ is always even. This statement is correct only in theories without scalar fields. In the $\mathcal{N} = 4$ theory, a pair of positive helicity fermions, Λ^{1+} , Λ^{2+} , can be connected to another pair of positive helicity fermions, Λ^{3+} , Λ^{4+} , by a scalar propagator.

In $\mathcal{N} \leq 1$ theory a tree amplitude A_n with less than two opposite helicities vanishes² identically [18]. First nonvanishing amplitudes contain $n - 2$ particles with helicities of the same sign [19, 20] and are called maximal helicity violating (MHV) amplitudes.

In the spinor helicity formalism [21, 19, 20] an on-shell momentum of a massless particle, $p_\mu p^\mu = 0$, is represented as

$$p_{a\dot{a}} \equiv p_\mu \sigma_{a\dot{a}}^\mu = \lambda_a \tilde{\lambda}_{\dot{a}} , \quad (1.1)$$

where λ_a and $\tilde{\lambda}_{\dot{a}}$ are two commuting spinors of positive and negative chirality. Spinor inner products are defined by³

$$\langle \lambda, \lambda' \rangle = \epsilon_{ab} \lambda^a \lambda'^b , \quad [\tilde{\lambda}, \tilde{\lambda}'] = \epsilon_{\dot{a}\dot{b}} \tilde{\lambda}^{\dot{a}} \tilde{\lambda}'^{\dot{b}} , \quad (1.2)$$

and a scalar product of two null vectors, $p_{a\dot{a}} = \lambda_a \tilde{\lambda}_{\dot{a}}$ and $q_{a\dot{a}} = \lambda'_a \tilde{\lambda}'_{\dot{a}}$, becomes

$$p_\mu q^\mu = \frac{1}{2} \langle \lambda, \lambda' \rangle [\tilde{\lambda}, \tilde{\lambda}'] . \quad (1.3)$$

An MHV amplitude $A_n = A_{l+2m}$ with l gluons and $2m$ fermions in $\mathcal{N} \leq 1$ theories exists only for $m = 0, 1, 2$. This is because it must have precisely $n - 2$ particles with positive and 2 with negative helicities, and our fermions always come in pairs with helicities $\pm\frac{1}{2}$. Hence, there are three types of MHV tree amplitudes in $\mathcal{N} \leq 1$ theories:

$$A_n(g_r^-, g_s^-) , \quad A_n(g_t^-, \Lambda_r^-, \Lambda_s^+) , \quad A_n(\Lambda_t^-, \Lambda_s^+, \Lambda_r^-, \Lambda_q^+) . \quad (1.4)$$

Suppressing the overall momentum conservation factor, $i g_{\text{YM}}^{n-2} (2\pi)^4 \delta^{(4)}(\sum_{i=1}^n \lambda_{i\dot{a}} \tilde{\lambda}_{i\dot{a}})$, the MHV purely gluonic amplitude reads [19, 20]:

$$A_n(g_r^-, g_s^-) = \frac{\langle \lambda_r, \lambda_s \rangle^4}{\prod_{i=1}^n \langle \lambda_i, \lambda_{i+1} \rangle} \equiv \frac{\langle r \ s \rangle^4}{\prod_{i=1}^n \langle i \ i+1 \rangle} , \quad (1.5)$$

²In the $\mathcal{N} = 1$ theory this is also correct to all orders in the loop expansion and non-perturbatively.

³Our conventions for spinor helicities follow [2, 1] and are the same as in [3].

where $\lambda_{n+1} \equiv \lambda_1$. The MHV amplitude with two external fermions and $n - 2$ gluons is

$$A_n(g_t^-, \Lambda_r^-, \Lambda_s^+) = \frac{\langle t r \rangle^3 \langle t s \rangle}{\prod_{i=1}^n \langle i i+1 \rangle}, \quad A_n(g_t^-, \Lambda_s^+, \Lambda_r^-) = - \frac{\langle t r \rangle^3 \langle t s \rangle}{\prod_{i=1}^n \langle i i+1 \rangle}, \quad (1.6)$$

where the first expression corresponds to $r < s$ and the second to $s < r$ (and t is arbitrary).

The MHV amplitudes with four fermions and $n - 4$ gluons on external lines are

$$A_n(\Lambda_t^-, \Lambda_s^+, \Lambda_r^-, \Lambda_q^+) = \frac{\langle t r \rangle^3 \langle s q \rangle}{\prod_{i=1}^n \langle i i+1 \rangle}, \quad A_n(\Lambda_t^-, \Lambda_r^-, \Lambda_s^+, \Lambda_q^+) = - \frac{\langle t r \rangle^3 \langle s q \rangle}{\prod_{i=1}^n \langle i i+1 \rangle} \quad (1.7)$$

The first expression in (1.7) corresponds to $t < s < r < q$, the second – to $t < r < s < q$, and there are other similar expressions, obtained by further permutations of fermions, with the overall sign determined by the ordering.

Expressions (1.6), (1.7) can be derived from supersymmetric Ward identities [18, 22, 23], and we will have more to say about this in section 5. The $\overline{\text{MHV}}$ amplitude can be obtained, as always, by exchanging helicities $+ \leftrightarrow -$ and $\langle i j \rangle \leftrightarrow [i j]$.

2. Gluonic NMHV amplitudes and the CSW method

The formalism of CSW was developed in [1] for calculating purely gluonic amplitudes at tree level. In this approach all non-MHV n -gluon amplitudes (including $\overline{\text{MHV}}$) are expressed as sums of tree diagrams in an effective scalar perturbation theory. The vertices in this theory are the MHV amplitudes (1.5), continued off-shell as described below, and connected by scalar propagators $1/q^2$.

It was shown in [3] that the same idea continues to work in theories with fermions and gluons. Scattering amplitudes are determined from scalar diagrams with three types of MHV vertices, (1.5), (1.6) and (1.7), which are connected to each other with scalar propagators $1/q^2$. Also, at tree level, supersymmetry is irrelevant and the method applies to supersymmetric and non-supersymmetric theories [3].

When one leg of an MHV vertex is connected by a propagator to a leg of another MHV vertex, both legs become internal to the diagram and have to be continued off-shell. Off-shell continuation is defined as follows [1]: we pick an arbitrary spinor $\xi_{\text{Ref}}^{\dot{a}}$ and define λ_a for any internal line carrying momentum $q_{a\dot{a}}$ by

$$\lambda_a = q_{a\dot{a}} \xi_{\text{Ref}}^{\dot{a}}. \quad (2.1)$$

External lines in a diagram remain on-shell, and for them λ is defined in the usual way. For the off-shell lines, the same ξ_{Ref} is used in all diagrams contributing to a given amplitude.

For practical applications the authors of [1] have chosen $\xi_{\text{Ref}}^{\dot{a}}$ in (2.1) to be equal to $\tilde{\lambda}^{\dot{a}}$ of one of the external legs of negative helicity, e.g. the first one,

$$\xi_{\text{Ref}} = \tilde{\lambda}_1^{\dot{a}}. \quad (2.2)$$

This corresponds to identifying the reference spinor with one of the kinematic variables of the theory. The explicit dependence on the reference spinor $\xi_{\text{Ref}}^{\dot{a}}$ disappears and the resulting expressions for all scalar diagrams in the CSW approach are the functions only of the kinematic variables $\lambda_{i a}$ and $\tilde{\lambda}_i^{\dot{a}}$. This means that the expressions for all individual diagrams automatically appear to be Lorentz-invariant (in the sense that they do not depend on an external spinor $\xi_{\text{Ref}}^{\dot{a}}$) and also gauge-invariant (since the reference spinor corresponds to the axial gauge fixing $n_{\mu} A^{\mu} = 0$, where $n_{a\dot{a}} = \xi_{\text{Ref} a} \xi_{\text{Ref} \dot{a}}$).

There is a price to pay for this invariance of the individual diagrams. Equations (2.1),(2.2) lead to unphysical singularities⁴ which occur for the whole of phase space and which have to be cancelled between the individual diagrams. The result for the total amplitude is, of course, free of these unphysical singularities, but their cancellation and the retention of the finite part requires some work, see [1] and section 3.1 of [3].

It will be important for the purposes of this paper to note that these unphysical singularities are specific to the three-gluon MHV vertices and, importantly, they do not occur in any of the MHV vertices involving a fermion field [3]. To see how these singularities arise in gluon vertices, consider a 3-point MHV vertex,

$$A_3(g_1^-, g_2^-, g_3^+) = \frac{\langle 1 2 \rangle^4}{\langle 1 2 \rangle \langle 2 3 \rangle \langle 3 1 \rangle} = \frac{\langle 1 2 \rangle^3}{\langle 2 3 \rangle \langle 3 1 \rangle}. \quad (2.3)$$

This vertex exists only when one of the legs is off-shell. Take it to be the g_3^+ leg. Then Eqs. (2.1), (2.2) give

$$\lambda_{3 a} = (p_1 + p_2) \tilde{\lambda}_1^{\dot{a}} = -\lambda_{1 a} [1 1] - \lambda_{2 a} [2 1] = -\lambda_{2 a} [2 1]. \quad (2.4)$$

This implies that $\langle 2 3 \rangle = -\langle 2 2 \rangle [2 1] = 0$, and the denominator of (2.3) vanishes. This is precisely the singularity we are after. If instead of the g_3^+ leg, one takes the g_2^- leg go off-shell, then, $\langle 2 3 \rangle = -\langle 3 3 \rangle [3 1] = 0$ again.

⁴Unphysical means that these singularities are not the standard IR soft and collinear divergences in the amplitudes.

Now consider a three-point MHV vertex involving two fermions and a gluon,

$$A_3(\Lambda_1^-, g_2^-, \Lambda_3^+) = \frac{\langle 2\ 1 \rangle^3 \langle 2\ 3 \rangle}{\langle 1\ 2 \rangle \langle 2\ 3 \rangle \langle 3\ 1 \rangle} = -\frac{\langle 2\ 1 \rangle^2}{\langle 3\ 1 \rangle}. \quad (2.5)$$

Choose the reference spinor to be as before, $\tilde{\lambda}_1^{\dot{a}}$, and take the second or the third leg off-shell. This again makes $\langle 2\ 3 \rangle = 0$, but now the factor of $\langle 2\ 3 \rangle$ is cancelled on the right hand side of (2.5). Hence, the vertex (2.5) is regular, and there are no unphysical singularities in the amplitudes involving at least one negative helicity fermion when it's helicity is chosen to be the reference spinor [3]. One concludes that the difficulties with singularities at intermediate stages of the calculation occur only in purely gluonic amplitudes. One way to avoid these intermediate singularities is to choose an off-shell continuation different from the CSW prescription (2.1),(2.2).

Very recently, Kosower [6] used an off-shell continuation by projection of the off-shell momentum with respect to an on-shell reference momentum q_{Ref}^μ , to derive, for the first time, an expression for a general NMHV amplitude with three negative helicity gluons. The amplitude in [6] was from the start free of unphysical divergences, however it required a certain amount of spinor algebra to bring it into the form independent of the reference momentum.

Here we will propose another simple method for finding all purely gluonic NMHV amplitudes. Using $\mathcal{N} = 1$ supersymmetric Ward identities one can relate purely gluonic amplitudes to a linear combination of amplitudes with one fermion–antifermion pair. As explained above, the latter are free of singularities and are manifestly Lorentz-invariant. These fermionic amplitudes will be calculated in the following section using the CSW scalar graph approach with fermions [3].

To derive supersymmetric Ward identities [18] we use the fact that, supercharges Q annihilate the vacuum, and consider the following equation,

$$\langle [Q, \Lambda_k^+ \dots g_{r_1}^- \dots g_{r_2}^- \dots g_{r_3}^- \dots] \rangle = 0, \quad (2.6)$$

where dots indicate positive helicity gluons. In order to make anticommuting spinor Q to be a singlet entering a commutative (rather than anticommutative) algebra with all the fields we contract it with a commuting spinor η and multiply it by a Grassmann number θ . This defines a commuting singlet operator $Q(\eta)$. Following [23] we can write down the following susy algebra relations,

$$\begin{aligned} [Q(\eta), \Lambda^+(k)] &= -\theta \langle \eta\ k \rangle g^+(k), & [Q(\eta), \Lambda^-(k)] &= +\theta [\eta\ k] g^-(k), \\ [Q(\eta), g^-(k)] &= +\theta \langle \eta\ k \rangle \Lambda^-(k), & [Q(\eta), g^+(k)] &= -\theta [\eta\ k] \Lambda^+(k). \end{aligned} \quad (2.7)$$

In what follows, the anticommuting parameter θ will cancel from the relevant expressions for the amplitudes. The arbitrary spinors $\eta_a, \eta_{\dot{a}}$, will be fixed below. It then follows from (2.7) that

$$\begin{aligned} \langle \eta k \rangle A_n(g_{r_1}^-, g_{r_2}^-, g_{r_3}^-) &= \langle \eta r_1 \rangle A_n(\Lambda_k^+, \Lambda_{r_1}^-, g_{r_2}^-, g_{r_3}^-) + \langle \eta r_2 \rangle A_n(\Lambda_k^+, g_{r_1}^-, \Lambda_{r_2}^-, g_{r_3}^-) \\ &\quad + \langle \eta r_3 \rangle A_n(\Lambda_k^+, g_{r_1}^-, g_{r_2}^-, \Lambda_{r_3}^-). \end{aligned} \quad (2.8)$$

After choosing η to be one of the three r_j we find from (2.8) that the purely gluonic amplitude with three negative helicities is given by a sum of two fermion-antifermion-gluon-gluon amplitudes. Note that in the expressions above and in what follows, in n -point amplitudes we show only the relevant particles, and suppress all the positive helicity gluons g^+ .

Remarkably, this approach works for any number of negative helicities, and the NMHV amplitude with h negative gluons is expressed via a simple linear combination of $h - 1$ NMHV amplitudes with one fermion-antifermion pair.

In sections 3 and 4 we will evaluate NMHV amplitudes with fermions. In particular, in section 3 we will calculate the following three amplitudes,

$$A_n(\Lambda_{m_1}^-, g_{m_2}^-, g_{m_3}^-, \Lambda_k^+), \quad A_n(\Lambda_{m_1}^-, g_{m_2}^-, \Lambda_k^+, g_{m_3}^-), \quad A_n(\Lambda_{m_1}^-, \Lambda_k^+, g_{m_2}^-, g_{m_3}^-). \quad (2.9)$$

In terms of these, the purely gluonic amplitude of (2.8) reads

$$\begin{aligned} A_n(g_{r_1}^-, g_{r_2}^-, g_{r_3}^-) &= -\frac{\langle \eta r_1 \rangle}{\langle \eta k \rangle} A_n(\Lambda_{m_1}^-, g_{m_2}^-, g_{m_3}^-, \Lambda_k^+) |_{m_1=r_1, m_2=r_2, m_3=r_3} \\ &\quad - \frac{\langle \eta r_2 \rangle}{\langle \eta k \rangle} A_n(\Lambda_{m_1}^-, g_{m_2}^-, \Lambda_k^+, g_{m_3}^-) |_{m_1=r_2, m_2=r_3, m_3=r_1} \\ &\quad - \frac{\langle \eta r_3 \rangle}{\langle \eta k \rangle} A_n(\Lambda_{m_1}^-, \Lambda_k^+, g_{m_2}^-, g_{m_3}^-) |_{m_1=r_3, m_2=r_1, m_3=r_2}, \end{aligned} \quad (2.10)$$

and η can be chosen to be one of the three m_j to further simplify this formula.

3. NMHV (- - -) Amplitudes with Two Fermions

We start with the case of one fermion-antifermion pair, Λ^-, Λ^+ , and an arbitrary number of gluons, g . The amplitude has a schematic form, $A_n(\Lambda_{m_1}^-, g_{m_2}^-, g_{m_3}^-, \Lambda_k^+)$, and without loss of generality we can have $m_1 < m_2 < m_3$. With these conventions, there are three different classes of amplitudes depending on the position of the Λ_k^+ fermion relative to m_1, m_2, m_3 :

$$A_n(\Lambda_{m_1}^-, g_{m_2}^-, g_{m_3}^-, \Lambda_k^+), \quad (3.1a)$$

$$A_n(\Lambda_{m_1}^-, g_{m_2}^-, \Lambda_k^+, g_{m_3}^-), \quad (3.1b)$$

$$A_n(\Lambda_{m_1}^-, \Lambda_k^+, g_{m_2}^-, g_{m_3}^-). \quad (3.1c)$$

Each of these three amplitudes receives contributions from different types of scalar diagrams in the CSW approach. In all of these scalar diagrams there are precisely two MHV vertices connected to each other by a single scalar propagator [1]. We will always arrange these diagrams in such a way that the MHV vertex on the left has a positive helicity on the internal line, and the right vertex has a negative helicity. Then, there are three choices one can make [6] for the pair of negative helicity particles to enter external lines of the left vertex, (m_1, m_2) , (m_2, m_3) , or (m_3, m_1) . In addition to this, each diagram in $\mathcal{N} \leq 1$ theory corresponds to either a gluon exchange, or a fermion exchange.

The diagrams contributing to the first process (3.1a) are drawn in Figure 1. There are three gluon exchange diagrams for all three partitions (m_2, m_3) , (m_1, m_2) , (m_3, m_1) , and there is one fermion exchange diagram for the partition (m_1, m_2) .

It is now straightforward, using the expressions for the MHV vertices (1.5),(1.6), to write down an analytic expression for the first diagram of Figure 1:

$$A_n^{(1)} = \frac{1}{\prod_{l=1}^n \langle l l+1 \rangle} \sum_{i=m_1}^{m_2-1} \sum_{j=m_3}^{k-1} \frac{-\langle (i+1, j) m_1 \rangle^3 \langle (i+1, j) k \rangle \langle i i+1 \rangle \langle j j+1 \rangle}{\langle i (i+1, j) \rangle \langle (i+1, j) j+1 \rangle q_{i+1, j}^2} \times \frac{\langle m_2 m_3 \rangle^4}{\langle (j+1, i) i+1 \rangle \langle j (j+1, i) \rangle} . \quad (3.2)$$

This expression is a direct rendering of the ‘Feynman rules’ for the scalar graph method [1, 3], followed by factoring out the overall factor of $(\prod_{l=1}^n \langle l l+1 \rangle)^{-1}$. The objects $(i+1, j)$ and $(j+1, i)$ appearing on the right hand side of (3.2) denote the spinors $\lambda_{i+1, j}$ and $\lambda_{j+1, i}$ corresponding to the off-shell momentum $q_{i+1, j}$

$$q_{i+1, j} \equiv p_{i+1} + p_{i+2} + \dots + p_j , \quad q_{j+1, i} \equiv p_{j+1} + p_{j+2} + \dots + p_i , \quad q_{i+1, j} + q_{j+1, i} = 0 \quad (3.3)$$

$$\lambda_{i+1, j a} \equiv q_{i+1, j a} \xi_{\text{Ref}}^{\dot{a}} = -\lambda_{j+1, i a} , \quad (3.4)$$

where $\xi_{\text{Ref}}^{\dot{a}}$ is the reference (dotted) spinor [1] as in Eq. (2.1). All other spinors λ_i are on-shell and $\langle i (j, k) \rangle$ is an abbreviation for a spinor product $\langle \lambda_i, \lambda_{jk} \rangle$.

Having the freedom to choose any reference spinor we will always choose it to be the spinor of the fermion Λ^- . In this section, this is the spinor of $\Lambda_{m_1}^-$,

$$\xi_{\text{Ref}} = \tilde{\lambda}_{m_1}^{\dot{a}} . \quad (3.5)$$

We can now re-write

$$\begin{aligned} & \langle i (i+1, j) \rangle \langle (i+1, j) j+1 \rangle \langle (j+1, i) i+1 \rangle \langle j (j+1, i) \rangle \\ & = \langle i^- | \not{q}_{i+1, j} | m_1^- \rangle \langle j+1^- | \not{q}_{i+1, j} | m_1^- \rangle \langle i+1^- | \not{q}_{i+1, j} | m_1^- \rangle \langle j^- | \not{q}_{i+1, j} | m_1^- \rangle , \end{aligned} \quad (3.6)$$

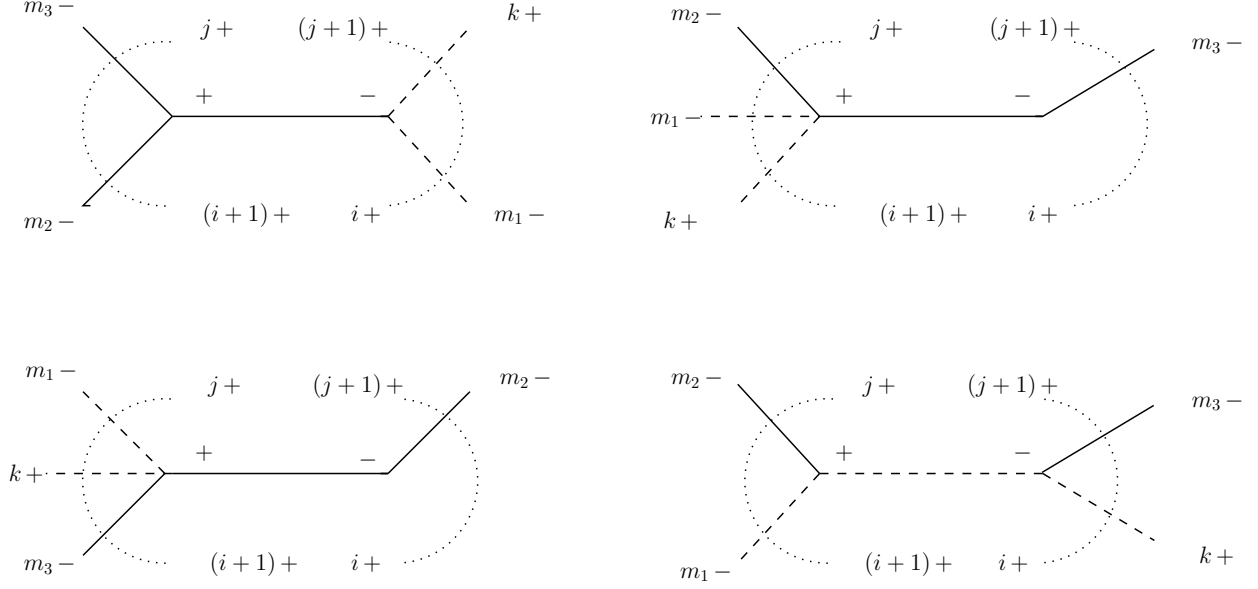


Figure 1: Tree diagrams with MHV vertices contributing to the amplitude $A_n(\Lambda_{m_1}^-, g_{m_2}^-, g_{m_3}^-, \Lambda_k^+)$. Fermions, Λ^+ and Λ^- , are represented by dashed lines and negative helicity gluons, g^- , by solid lines. Positive helicity gluons g^+ emitted from each vertex are indicated by dotted semicircles with labels showing the bounding g^+ lines in each MHV vertex.

and define a universal combination,

$$D = \langle i^- | \not{p}_{i+1,j} | m_1^- \rangle \langle j+1^- | \not{p}_{i+1,j} | m_1^- \rangle \langle i+1^- | \not{p}_{i+1,j} | m_1^- \rangle \langle j^- | \not{p}_{i+1,j} | m_1^- \rangle \frac{q_{i+1,j}^2}{\langle i \ i+1 \rangle \langle j \ j+1 \rangle} \quad (3.7)$$

Note that Here we introduced the standard Lorentz-invariant matrix element $\langle i^- | \not{p}_k | j^- \rangle = i^a p_k{}_{a\dot{a}} j^{\dot{a}}$, which in terms of the spinor products is

$$\langle i^- | \not{p}_k | j^- \rangle = \langle i^- |^a | k^+ \rangle_a \langle k^+ |_{\dot{a}} | j^- \rangle^{\dot{a}} = -\langle i \ k \rangle [k \ j] = \langle i \ k \rangle [j \ k]. \quad (3.8)$$

The expression for $A_n^{(1)}$ now becomes:

$$A_n^{(1)} = \frac{-1}{\prod_{l=1}^n \langle l \ l+1 \rangle} \sum_{i=m_1}^{m_2-1} \sum_{j=m_3}^{k-1} \frac{\langle m_1^- | \not{p}_{i+1,j} | m_1^- \rangle^3 \langle k^- | \not{p}_{i+1,j} | m_1^- \rangle \langle m_2 \ m_3 \rangle^4}{D}. \quad (3.9)$$

For the second diagram of Figure 1, we have

$$A_n^{(2)} = \frac{-1}{\prod_{l=1}^n \langle l \ l+1 \rangle} \sum_{i=m_3}^{k-1} \sum_{j=m_2}^{m_3-1} \frac{\langle m_3^- | \not{p}_{i+1,j} | m_1^- \rangle^4 \langle m_2 \ m_1 \rangle^3 \langle m_2 \ k \rangle}{D}. \quad (3.10)$$

The MHV vertex on the right in the second diagram in Figure 1 can collapse to a 2-leg vertex. This occurs when $i = m_3$ and $j + 1 = m_3$. This vertex is identically zero, since $q_{j+1,i} = p_{m_3} = -q_{i+1,j}$, and $\langle m_3 m_3 \rangle = 0$. Similar considerations apply in (3.11), (3.15), (3.17), (3.20), (3.21), (4.3) and (4.11).

Expressions corresponding to the third and fourth diagrams in Figure 1 are

$$A_n^{(3)} = \frac{-1}{\prod_{l=1}^n \langle l l+1 \rangle} \sum_{i=m_2}^{m_3-1} \sum_{j=m_1}^{m_2-1} \frac{\langle m_2^- | \not{q}_{i+1,j} | m_1^- \rangle^4 \langle m_3 m_1 \rangle^3 \langle m_3 k \rangle}{D}, \quad (3.11)$$

$$A_n^{(4)} = \frac{-1}{\prod_{l=1}^n \langle l l+1 \rangle} \sum_{i=k}^{n+m_1-1} \sum_{j=m_2}^{m_3-1} \frac{\langle m_3^- | \not{q}_{i+1,j} | m_1^- \rangle^3 \langle m_2^- | \not{q}_{i+1,j} | m_1^- \rangle \langle m_2 m_1 \rangle^3 \langle m_3 k \rangle}{D}. \quad (3.12)$$

Note that the first sum in (3.12), $\sum_{i=k}^{n+m_1-1}$, is understood to run in cyclic order, for example $\sum_{i=4}^3 = \sum_{i=4,\dots,n,1,2,3}$. The same comment will also apply to similar sums in Eqs. (3.14), (3.17), (3.19), (3.20) below.

The total amplitude is the sum of (3.9), (3.10), (3.11) and (3.12),

$$A_n(\Lambda_{m_1}^-, g_{m_2}^-, g_{m_3}^-, \Lambda_k^+) = \sum_{i=1}^4 A_n^{(i)}. \quad (3.13)$$

There are three sources of zeroes in the denominator combination D defined in (3.7). First, there are genuine zeroes in, for example, $\langle i^- | \not{q}_{i+1,j} | m_1^- \rangle$ when $q_{i+1,j}$ is proportional to p_i . This occurs when $j = i-1$. Such terms are always associated with two-leg vertices as discussed above and produce zeroes in the numerator. In fact, the number of zeroes in the numerator always exceeds the number of zeroes in the denominator and this contribution vanishes. Second, there are zeroes associated with three-point vertices when, for example, $i = m_2$ and $q_{i+1,j} = p_{m_2} + p_{m_1}$ so that $\langle m_2^- | \not{\eta}_{l_1} + \not{\eta}_{l_2} | m_1^- \rangle = 0$. As discussed in Sec. 2, there is always a compensating factor in the numerator. Such terms give a finite contribution (see (2.5)). Third, there are accidental zeroes when $q_{i+1,j}$ happens to be a linear combination of p_i and p_{m_1} . For general phase space points this is not the case. However, at certain phase space points, the Gram determinant of p_i , p_{m_1} and $q_{i+1,j}$ does vanish. This produces an apparent singularity in individual terms in (3.9)–(3.12) which cancels when all contributions are taken into account. This cancellation can be achieved numerically or straightforwardly eliminated using standard spinor techniques [6].

For the special case of coincident negative helicities, $m_1 = 1$, $m_2 = 2$, $m_3 = 3$, the double sums in Eqs. (3.9)–(3.12) collapse to single sums. Furthermore, we see that the contribution from (3.11) vanishes due to momentum conservation, $q_{2,1} = 0$. The remaining three terms agree with the result presented in Eq. (3.6) of Ref. [3].

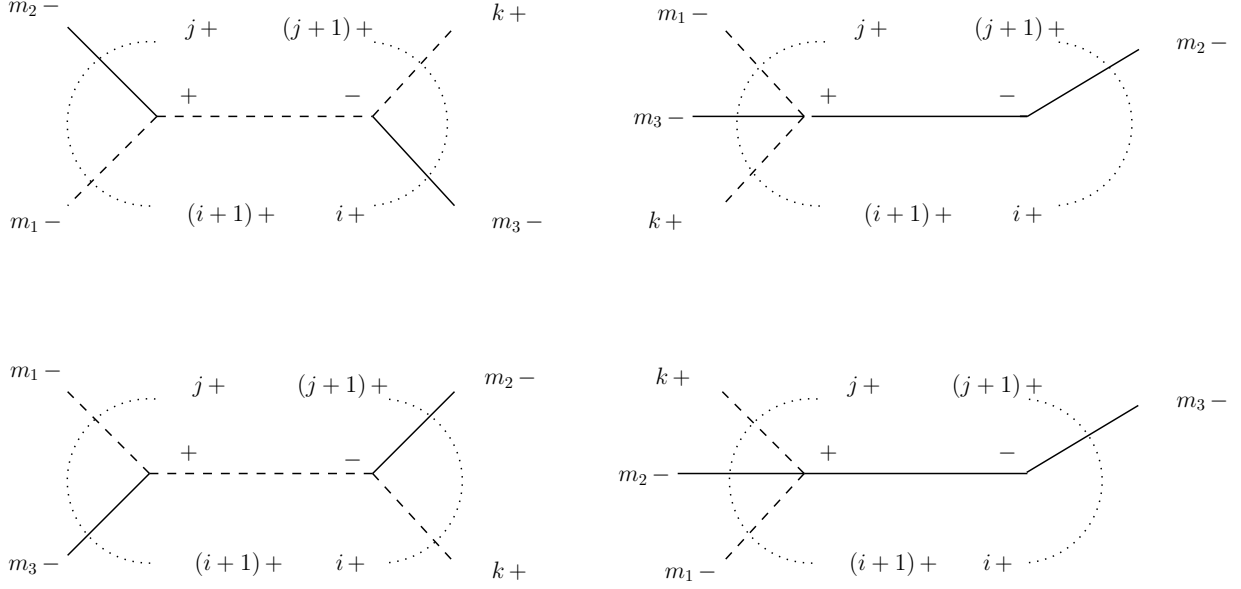


Figure 2: Tree diagrams with MHV vertices contributing to the amplitude $A_n(\Lambda_{m_1}^-, g_{m_2}^-, \Lambda_k^+, g_{m_3}^-)$.

We now consider the second amplitude, Eq. (3.1b). The scalar graph diagrams are shown in Figure 2. There is a fermion exchange and a gluon exchange diagram for two of the line assignments, (m_1, m_2) , and (m_3, m_1) , and none for the remaining assignment (m_2, m_3) .

These four diagrams result in:

$$A_n^{(1)'} = \frac{1}{\prod_{l=1}^n \langle l \ l+1 \rangle} \sum_{i=m_3}^{n+m_1-1} \sum_{j=m_2}^{k-1} \frac{\langle m_3^- | \not{q}_{i+1,j} | m_1^- \rangle^3 \langle m_2^- | \not{q}_{i+1,j} | m_1^- \rangle \langle m_2 \ m_1 \rangle^3 \langle m_3 \ k \rangle}{D} \quad (3.14)$$

$$A_n^{(2)'} = \frac{1}{\prod_{l=1}^n \langle l \ l+1 \rangle} \sum_{i=m_2}^{k-1} \sum_{j=m_1}^{m_2-1} \frac{\langle m_2^- | \not{q}_{i+1,j} | m_1^- \rangle^4 \langle m_3 \ m_1 \rangle^3 \langle m_3 \ k \rangle}{D}, \quad (3.15)$$

$$A_n^{(3)'} = \frac{1}{\prod_{l=1}^n \langle l \ l+1 \rangle} \sum_{i=k}^{m_3-1} \sum_{j=m_1}^{m_2-1} \frac{\langle m_2^- | \not{q}_{i+1,j} | m_1^- \rangle^3 \langle m_3^- | \not{q}_{i+1,j} | m_1^- \rangle \langle m_3 \ m_1 \rangle^3 \langle m_2 \ k \rangle}{D}, \quad (3.16)$$

$$A_n^{(4)'} = \frac{-1}{\prod_{l=1}^n \langle l \ l+1 \rangle} \sum_{i=m_3}^{n+m_1-1} \sum_{j=k}^{m_3-1} \frac{\langle m_3^- | \not{q}_{i+1,j} | m_1^- \rangle^4 \langle m_2 \ m_1 \rangle^3 \langle m_2 \ k \rangle}{D}, \quad (3.17)$$

and the final answer for (3.1b) is,

$$A_n(\Lambda_{m_1}^-, g_{m_2}^-, \Lambda_k^+, g_{m_3}^-) = \sum_{i=1}^4 A_n^{(i)'}. \quad (3.18)$$

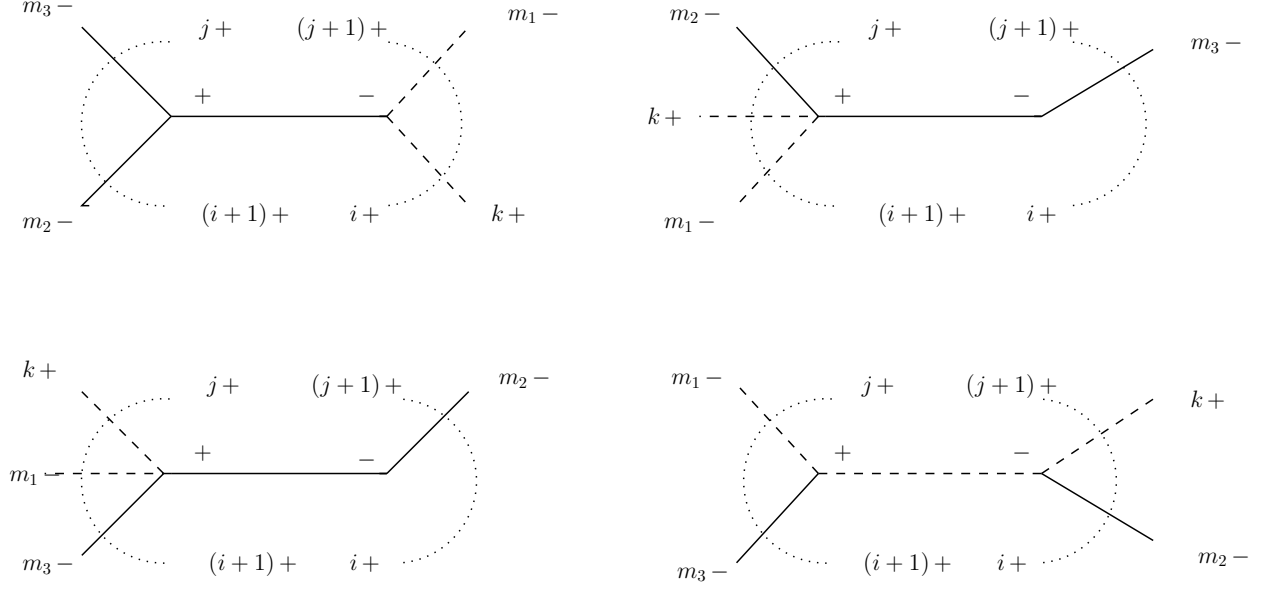


Figure 3: Tree diagrams with MHV vertices contributing to the amplitude $A_n(\Lambda_{m_1}^-, \Lambda_k^+, g_{m_2}^-, g_{m_3}^-)$.

Finally, we give the result for (3.1c). The corresponding diagrams are drawn in Figure 3. We find

$$A_n^{(1)''} = \frac{1}{\prod_{l=1}^n \langle l \ l+1 \rangle} \sum_{i=k}^{m_2-1} \sum_{j=m_3}^{n+m_1-1} \frac{\langle m_1^- | \not{q}_{i+1,j} | m_1^- \rangle^3 \langle k^- | \not{q}_{i+1,j} | m_1^- \rangle \langle m_2 \ m_3 \rangle^4}{D}, \quad (3.19)$$

$$A_n^{(2)''} = \frac{1}{\prod_{l=1}^n \langle l \ l+1 \rangle} \sum_{i=m_3}^{n+m_1-1} \sum_{j=m_2}^{m_3-1} \frac{\langle m_3^- | \not{q}_{i+1,j} | m_1^- \rangle^4 \langle m_2 \ m_1 \rangle^3 \langle m_2 \ k \rangle}{D}, \quad (3.20)$$

$$A_n^{(3)''} = \frac{1}{\prod_{l=1}^n \langle l \ l+1 \rangle} \sum_{i=m_2}^{m_3-1} \sum_{j=k}^{m_2-1} \frac{\langle m_2^- | \not{q}_{i+1,j} | m_1^- \rangle^4 \langle m_3 \ m_1 \rangle^3 \langle m_3 \ k \rangle}{D}, \quad (3.21)$$

$$A_n^{(4)''} = \frac{-1}{\prod_{l=1}^n \langle l \ l+1 \rangle} \sum_{i=m_2}^{m_3-1} \sum_{j=m_1}^{k-1} \frac{\langle m_2^- | \not{q}_{i+1,j} | m_1^- \rangle^3 \langle m_3^- | \not{q}_{i+1,j} | m_1^- \rangle \langle m_3 \ m_1 \rangle^3 \langle m_2 \ k \rangle}{D}. \quad (3.22)$$

As before, the full amplitude is given by the sum of contributions,

$$A_n(\Lambda_{m_1}^-, \Lambda_k^+, g_{m_2}^-, g_{m_3}^-) = \sum_{i=1}^4 A_n^{(i)''}. \quad (3.23)$$

4. NMHV (- - -) Amplitudes with Four Fermions

We now consider the amplitudes with 2 fermion-antifermion lines. In what follows, without loss of generality we will choose the negative helicity gluon to be the first particle. With this convention, we can write the six inequivalent amplitudes as:

$$A_n(g_1^-, \Lambda_{m_2}^-, \Lambda_{m_3}^-, \Lambda_{m_p}^+, \Lambda_{m_q}^+) , \quad (4.1a)$$

$$A_n(g_1^-, \Lambda_{m_2}^-, \Lambda_{m_p}^+, \Lambda_{m_3}^-, \Lambda_{m_q}^+) , \quad (4.1b)$$

$$A_n(g_1^-, \Lambda_{m_2}^-, \Lambda_{m_p}^+, \Lambda_{m_q}^+, \Lambda_{m_3}^-) , \quad (4.1c)$$

$$A_n(g_1^-, \Lambda_{m_p}^+, \Lambda_{m_2}^-, \Lambda_{m_3}^-, \Lambda_{m_q}^+) , \quad (4.1d)$$

$$A_n(g_1^-, \Lambda_{m_p}^+, \Lambda_{m_2}^-, \Lambda_{m_q}^+, \Lambda_{m_3}^-) , \quad (4.1e)$$

$$A_n(g_1^-, \Lambda_{m_p}^+, \Lambda_{m_q}^+, \Lambda_{m_2}^-, \Lambda_{m_3}^-) . \quad (4.1f)$$

The calculation of the amplitudes of (4.1a)-(4.1f) is straightforward. The diagrams contributing to the first process are shown in Figure 4. It should be noted that not all the amplitudes in (4.1a)-(4.1f) receive contributions from the same number of diagrams. For example, there are four diagrams for the process of (4.1a) while there are six for that of (4.1b). In order to avoid vanishing denominators, one can choose the reference spinor to be $\tilde{\eta} = \tilde{\lambda}_{m_2}$. With this

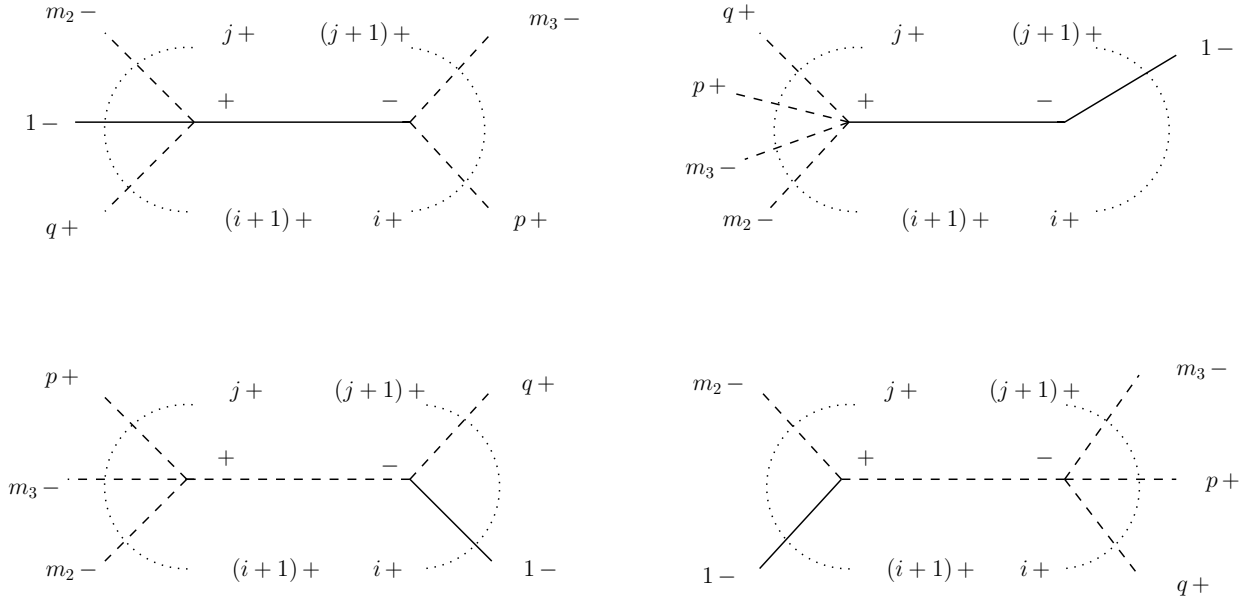


Figure 4: Tree diagrams with MHV vertices contributing to the four fermion amplitude $A_n(g_1^-, \Lambda_{m_2}^-, \Lambda_{m_3}^-, \Lambda_{m_p}^+, \Lambda_{m_q}^+)$.

choice the result can be written as:

$$\tilde{A}_n^{(1)} = \frac{1}{\prod_{l=1}^n \langle l \ l+1 \rangle} \sum_{i=p}^{q-1} \sum_{j=m_2}^{m_3-1} \frac{\langle m_3^- | \not{q}_{i+1,j} | m_2^- \rangle^3 \langle p^- | \not{q}_{i+1,j} | m_2^- \rangle \langle 1 \ m_2 \rangle^3 \langle 1 \ q \rangle}{D}, \quad (4.2)$$

$$\tilde{A}_n^{(2)} = \frac{-1}{\prod_{l=1}^n \langle l \ l+1 \rangle} \sum_{i=1}^{m_2-1} \sum_{j=q}^n \frac{\langle 1^- | \not{q}_{i+1,j} | m_2^- \rangle^4 \langle m_2 \ m_3 \rangle^3 \langle p \ q \rangle}{D}, \quad (4.3)$$

$$\tilde{A}_n^{(3)} = \frac{1}{\prod_{l=1}^n \langle l \ l+1 \rangle} \sum_{i=1}^{m_2-1} \sum_{j=p}^{q-1} \frac{\langle 1^- | \not{q}_{i+1,j} | m_2^- \rangle^3 \langle p^- | \not{q}_{i+1,j} | m_2^- \rangle \langle m_2 \ m_3 \rangle^3 \langle 1 \ q \rangle}{D}, \quad (4.4)$$

$$\tilde{A}_n^{(4)} = \frac{-1}{\prod_{l=1}^n \langle l \ l+1 \rangle} \sum_{i=q}^n \sum_{j=m_2}^{m_3-1} \frac{\langle m_3^- | \not{q}_{i+1,j} | m_2^- \rangle^3 \langle 1^- | \not{q}_{i+1,j} | m_2^- \rangle \langle 1 \ m_2 \rangle^3 \langle p \ q \rangle}{D}. \quad (4.5)$$

As before the final result is the sum of Eq. (4.2)-(4.5).

$$A_n(g_1^-, \Lambda_{m_2}^-, \Lambda_{m_3}^-, \Lambda_{m_p}^+, \Lambda_{m_q}^+) = \sum_{i=1}^4 \tilde{A}_n^{(i)}. \quad (4.6)$$

Once again, for the case of coincident negative helicities, $m_2 = 2$, $m_3 = 3$, the double sums collapse to single summations and we recover the results given in Ref. [3].

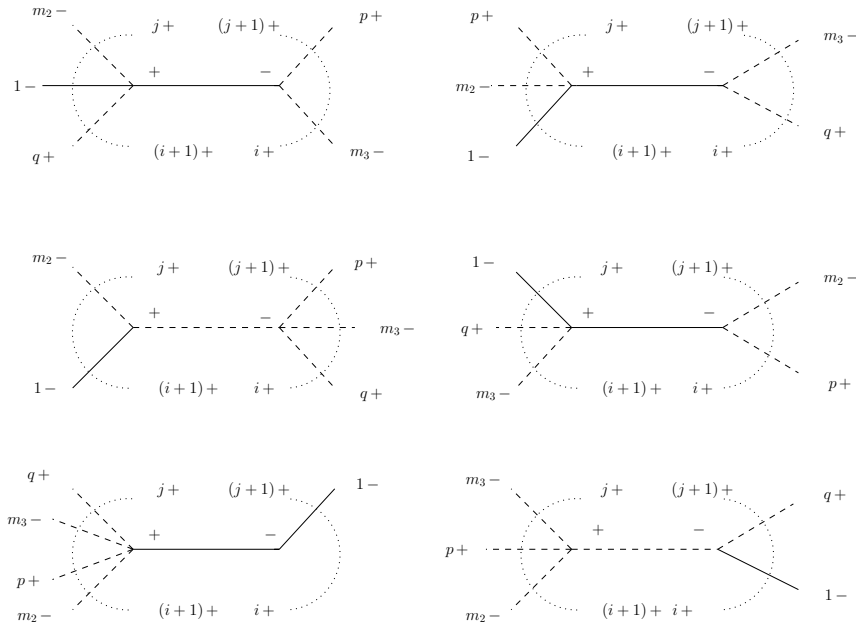


Figure 5: Tree diagrams with MHV vertices contributing to the four fermion amplitude $A_n(g_1^-, \Lambda_{m_2}^-, \Lambda_{m_p}^+, \Lambda_{m_3}^-, \Lambda_{m_q}^+)$.

As a last example we write down the expression for the amplitude of (4.1b). The corresponding diagrams are shown in Figure 5. We find,

$$\tilde{A}_n^{(1)'} = \frac{-1}{\prod_{l=1}^n \langle l \ l + 1 \rangle} \sum_{i=m_3}^{q-1} \sum_{j=m_2}^{p-1} \frac{\langle m_3^- | \not{q}_{i+1,j} | m_2^- \rangle^3 \langle p^- | \not{q}_{i+1,j} | m_2^- \rangle \langle 1 \ m_2 \rangle^3 \langle 1 \ q \rangle}{D}, \quad (4.7)$$

$$\tilde{A}_n^{(2)'} = \frac{1}{\prod_{l=1}^n \langle l \ l + 1 \rangle} \sum_{i=q}^n \sum_{j=p}^{m_3-1} \frac{\langle m_3^- | \not{q}_{i+1,j} | m_2^- \rangle^3 \langle q^- | \not{q}_{i+1,j} | m_2^- \rangle \langle 1 \ m_2 \rangle^3 \langle 1 \ p \rangle}{D}, \quad (4.8)$$

$$\tilde{A}_n^{(3)'} = \frac{1}{\prod_{l=1}^n \langle l \ l + 1 \rangle} \sum_{i=q}^n \sum_{j=m_2}^{p-1} \frac{\langle m_3^- | \not{q}_{i+1,j} | m_2^- \rangle^3 \langle 1^- | \not{q}_{i+1,j} | m_2^- \rangle \langle 1 \ m_2 \rangle^3 \langle p \ q \rangle}{D}, \quad (4.9)$$

$$\tilde{A}_n^{(4)'} = \frac{1}{\prod_{l=1}^n \langle l \ l + 1 \rangle} \sum_{i=p}^{m_3-1} \sum_{j=1}^{m_2-1} \frac{\langle m_2^- | \not{q}_{i+1,j} | m_2^- \rangle^3 \langle p^- | \not{q}_{i+1,j} | m_2^- \rangle \langle 1 \ m_3 \rangle^3 \langle 1 \ q \rangle}{D}, \quad (4.10)$$

$$\tilde{A}_n^{(5)'} = \frac{1}{\prod_{l=1}^n \langle l \ l + 1 \rangle} \sum_{i=1}^{m_2-1} \sum_{j=q}^n \frac{\langle 1^- | \not{q}_{i+1,j} | m_2^- \rangle^4 \langle m_2 \ m_3 \rangle^3 \langle p \ q \rangle}{D}, \quad (4.11)$$

$$\tilde{A}_n^{(6)'} = \frac{-1}{\prod_{l=1}^n \langle l \ l + 1 \rangle} \sum_{i=1}^{m_2-1} \sum_{j=m_3}^{q-1} \frac{\langle 1^- | \not{q}_{i+1,j} | m_2^- \rangle^3 \langle p^- | \not{q}_{i+1,j} | m_2^- \rangle \langle m_2 \ m_3 \rangle^3 \langle 1 \ q \rangle}{D}. \quad (4.12)$$

The full amplitude is the sum of Eq. (4.2)-(4.5).

$$A_n(g_1^-, \Lambda_{m_2}^-, \Lambda_{m_p}^+, \Lambda_{m_3}^-, \Lambda_{m_q}^+) = \sum_{i=1}^6 \tilde{A}_n^{(i)'}. \quad (4.13)$$

We close this section by listing the inequivalent NMHV amplitudes with three fermion–antifermion pairs. There are ten such amplitudes since choosing the first particle to be a negative helicity fermion we are left with five fermions (two of which have negative helicity and three positive) which should be distributed in all possible ways among themselves, and, in addition there are $(n - 6)$ positive helicity gluons. Thus the number of different possible ways is $5!$. However, the order of the particles of the same helicity is immaterial (since one can always choose $m_2 \leq m_3$ and $m_p \leq m_q \leq m_r$). This means that we have to divide $5!$ by $3!$ (for the positive helicity fermions) and by $2!$ (for the negative helicity fermions.) Thus there are ten different fermion amplitudes. These are listed below:

$$\begin{aligned} & A_n(\Lambda_1^-, \Lambda_{m_2}^-, \Lambda_{m_3}^-, \Lambda_{m_p}^+, \Lambda_{m_q}^+, \Lambda_{m_r}^+), \quad A_n(\Lambda_1^-, \Lambda_{m_2}^-, \Lambda_{m_p}^+, \Lambda_{m_3}^-, \Lambda_{m_q}^+, \Lambda_{m_r}^+), \\ & A_n(\Lambda_1^-, \Lambda_{m_2}^-, \Lambda_{m_p}^+, \Lambda_{m_q}^+, \Lambda_{m_3}^-, \Lambda_{m_r}^+), \quad A_n(\Lambda_1^-, \Lambda_{m_p}^+, \Lambda_{m_2}^-, \Lambda_{m_3}^-, \Lambda_{m_q}^+, \Lambda_{m_r}^+), \\ & A_n(\Lambda_1^-, \Lambda_{m_p}^+, \Lambda_{m_2}^-, \Lambda_{m_q}^+, \Lambda_{m_3}^-, \Lambda_{m_r}^+), \quad A_n(\Lambda_1^-, \Lambda_{m_p}^+, \Lambda_{m_q}^+, \Lambda_{m_2}^-, \Lambda_{m_3}^-, \Lambda_{m_r}^+), \\ & A_n(\Lambda_1^-, \Lambda_{m_p}^+, \Lambda_{m_q}^+, \Lambda_{m_r}^+, \Lambda_{m_2}^-, \Lambda_{m_3}^-), \quad A_n(\Lambda_1^-, \Lambda_{m_p}^+, \Lambda_{m_q}^+, \Lambda_{m_2}^-, \Lambda_{m_r}^+, \Lambda_{m_3}^-), \\ & A_n(\Lambda_1^-, \Lambda_{m_p}^+, \Lambda_{m_2}^-, \Lambda_{m_q}^+, \Lambda_{m_r}^+, \Lambda_{m_3}^-), \quad A_n(\Lambda_1^-, \Lambda_{m_2}^-, \Lambda_{m_p}^+, \Lambda_{m_q}^+, \Lambda_{m_r}^+, \Lambda_{m_3}^-). \end{aligned} \quad (4.14)$$

These amplitudes also present no difficulty, and they can be evaluated in the same manner as before.

5. Iterations of the Analytic Supervertex

5.1 Analytic Supervertex

So far we have encountered three types of MHV amplitudes (1.5), (1.6) and (1.7). The key feature which distinguishes these amplitudes is the fact that they depend only on $\langle \lambda_i \lambda_j \rangle$ spinor products, and not on $[\tilde{\lambda}_i \tilde{\lambda}_i]$. We will call such amplitudes analytic.

All analytic amplitudes in generic $0 \leq \mathcal{N} \leq 4$ gauge theories can be combined into a single $\mathcal{N} = 4$ supersymmetric expression of Nair [17],

$$A_n^{\mathcal{N}=4} = \delta^{(8)} \left(\sum_{i=1}^n \lambda_{ia} \eta_i^A \right) \frac{1}{\prod_{i=1}^n \langle i \ i+1 \rangle} . \quad (5.1)$$

Here η_i^A are anticommuting variables and $A = 1, 2, 3, 4$. The Grassmann-valued delta function is defined in the usual way,

$$\delta^{(8)} \left(\sum_{i=1}^n \lambda_{ia} \eta_i^A \right) \equiv \prod_{A=1}^4 \frac{1}{2} \left(\sum_{i=1}^n \lambda_i^a \eta_i^A \right) \left(\sum_{i=1}^n \lambda_{ia} \eta_i^A \right) , \quad (5.2)$$

where we have inserted factors of $\frac{1}{2}$ for future convenience. Taylor expanding (5.1) in powers of η_i , one can identify each term in the expansion with a particular tree-level analytic amplitude in the $\mathcal{N} = 4$ theory. $(\eta_i)^k$ for $k = 0, \dots, 4$ is interpreted as the i^{th} particle with helicity $h_i = 1 - \frac{k}{2}$. This implies that helicities take values, $\{1, \frac{1}{2}, 0, -\frac{1}{2}, -1\}$, which precisely correspond to those of the $\mathcal{N} = 4$ supermultiplet, $\{g^-, \lambda_A^-, \phi^{AB}, \Lambda^{A+}, g^+\}$.

It is straightforward to write down a general rule [3] for associating a power of η with all component fields in $\mathcal{N} = 4$,

$$\begin{aligned} g_i^- &\sim \eta_i^1 \eta_i^2 \eta_i^3 \eta_i^4 , & \phi_i^{AB} &\sim \eta_i^A \eta_i^B , & \Lambda_i^{A+} &\sim \eta_i^A , & g_i^+ &\sim 1 , \\ \Lambda_{1^-}^- &\sim -\eta_i^2 \eta_i^3 \eta_i^4 , & \Lambda_{2^-}^- &\sim -\eta_i^1 \eta_i^3 \eta_i^4 , & \Lambda_{3^-}^- &\sim -\eta_i^1 \eta_i^2 \eta_i^4 , & \Lambda_{4^-}^- &\sim -\eta_i^1 \eta_i^2 \eta_i^3 . \end{aligned} \quad (5.3)$$

The first MHV amplitude (1.5) is derived from (5.1) by using the dictionary (5.3) and by selecting the $(\eta_r)^4 (\eta_s)^4$ term in (5.1). The second amplitude (1.6) follows from the $(\eta_t)^4 (\eta_r)^3 (\eta_s)^1$ term in (5.1); and the third amplitude (1.7) is an $(\eta_r)^3 (\eta_s)^1 (\eta_p)^3 (\eta_q)^1$ term.

All amplitudes following from (5.1) are analytic in the sense that they depend only on $\langle \lambda_i \lambda_j \rangle$ spinor products, and not on $[\tilde{\lambda}_i \tilde{\lambda}_j]$. There is a large number of such component amplitudes for an extended susy Yang-Mills, and what is remarkable, not all of these amplitudes are MHV. The analytic amplitudes of the $\mathcal{N} = 4$ SYM obtained from (5.1), (5.3) are

$$\begin{aligned}
& A_n(g^-, g^-), \quad A_n(g^-, \Lambda_A^-, \Lambda^{A+}), \quad A_n(\Lambda_A^-, \Lambda_B^-, \Lambda^{A+}, \Lambda^{B+}), \\
& A_n(g^-, \Lambda^{1+}, \Lambda^{2+}, \Lambda^{3+}, \Lambda^{4+}), \quad A_n(\Lambda_A^-, \Lambda^{A+}, \Lambda^{1+}, \Lambda^{2+}, \Lambda^{3+}, \Lambda^{4+}), \\
& A_n(\Lambda^{1+}, \Lambda^{2+}, \Lambda^{3+}, \Lambda^{4+}, \Lambda^{1+}, \Lambda^{2+}, \Lambda^{3+}, \Lambda^{4+}), \quad A_n(\bar{\phi}_{AB}, \Lambda^{A+}, \Lambda^{B+}, \Lambda^{1+}, \Lambda^{2+}, \Lambda^{3+}, \Lambda^{4+}), \\
& A_n(g^-, \bar{\phi}_{AB}, \phi^{AB}), \quad A_n(g^-, \bar{\phi}_{AB}, \Lambda^{A+}, \Lambda^{B+}), \quad A_n(\Lambda_A^-, \Lambda_B^-, \phi^{AB}), \\
& A_n(\Lambda_A^-, \phi^{AB}, \bar{\phi}_{BC}, \Lambda^{C+}), \quad A_n(\Lambda_A^-, \bar{\phi}_{AB}, \Lambda^{A+}, \Lambda^{B+}, \Lambda^{C+}), \\
& A_n(\bar{\phi}, \phi, \bar{\phi}, \phi), \quad A_n(\bar{\phi}, \phi, \bar{\phi}, \Lambda^+, \Lambda^+), \quad A_n(\bar{\phi}, \bar{\phi}, \Lambda^+, \Lambda^+, \Lambda^+, \Lambda^+),
\end{aligned} \tag{5.4}$$

where it is understood that $\bar{\phi}_{AB} = \frac{1}{2}\epsilon_{ABCD}\phi^{CD}$. In Eqs. (5.4) we do not distinguish between the different particle orderings in the amplitudes. The labels refer to supersymmetry multiplets, $A, B = 1, \dots, 4$. Analytic amplitudes in (5.4) include the familiar MHV amplitudes, (1.5), (1.6), (1.7), as well as more complicated classes of amplitudes with external gluinos $\Lambda^A, \Lambda^{B \neq A}$, etc, and with external scalar fields ϕ^{AB} .

The second and third lines in (5.4) are not even MHV amplitudes, they have less than two negative helicities, and nevertheless, these amplitudes are non-vanishing in $\mathcal{N} = 4$ SYM.

All the analytic amplitudes listed in (5.4) can be calculated directly from (5.1), (5.3). There is a simple algorithm for doing this.

1. For each amplitude in (5.4) substitute the fields by their η -expressions (5.3). There are precisely eight η 's for each analytic amplitude.
2. Keeping track of the overall sign, rearrange the anticommuting η 's into a product of four pairs: $(\text{sign}) \times \eta_i^1 \eta_j^1 \eta_k^2 \eta_l^2 \eta_m^3 \eta_n^3 \eta_r^4 \eta_s^4$.
3. The amplitude is obtained by replacing each pair $\eta_i^A \eta_j^A$ by the spinor product $\langle i j \rangle$ and dividing by the usual denominator,

$$A_n = (\text{sign}) \times \frac{\langle i j \rangle \langle k l \rangle \langle m n \rangle \langle r s \rangle}{\prod_{l=1}^n \langle l l + 1 \rangle}. \tag{5.5}$$

5.2 Scalar graphs with analytic vertices

The conclusion we draw from the previous section is that in the scalar graph formalism in

$\mathcal{N} \leq 4$ SYM, the amplitudes are characterised not by a number of negative helicities, but rather by the total number of η 's associated to each amplitude via the rules (5.3).

The vertices of the scalar graph method are the analytic vertices (5.4) which are all of degree-8 in η . These vertices are analytic (they depend only on $\langle i j \rangle$ spinor products) and not necessarily MHV. These are component vertices of a single analytic supervertex⁵ (5.1). The analytic amplitudes are of degree-8 and they are the elementary blocks of the scalar graph approach. The next-to-minimal case are the amplitudes of degree-12 in η , and they are obtained by connecting two analytic vertices [17] with a scalar propagator $1/q^2$. Each analytic vertex contributes 8 η 's and a propagator removes 4. Scalar diagrams with three degree-8 vertices give the degree-12 amplitude, etc. In general, all n -point amplitudes are characterised by a degree $8, 12, 16, \dots, (4n-8)$ which are obtained from scalar diagrams with $1, 2, 3, \dots$ analytic vertices.⁶ In the next section we derive a simple expression for the first iteration of the degree-8 vertex. This iterative process can be continued straightforwardly to higher orders.

5.3 Two analytic supervertices

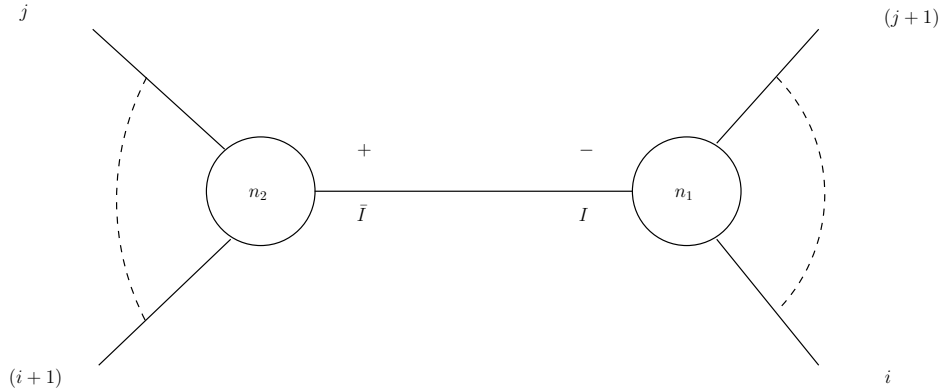


Figure 6: Tree diagrams with MHV vertices contributing to the first amplitude of Eq. (4.1b).

We now consider a diagram with two analytic supervertices (5.1) connected to one another by a single scalar propagator. The diagram is depicted in Figure 6. We follow the same conventions as in the previous sections, and the left vertex has a positive helicity on the internal line \bar{I} , while the right vertex has a negative helicity on the internal line I . The labelling

⁵The list of component vertices (5.4) is obtained by writing down all partitions of 8 into groups of 4, 3, 2 and 1. For example, $A_n(g^-, \bar{\phi}_{AB}, \Lambda^{A+}, \Lambda^{B+})$ follows from $8 = 4 + 2 + 1 + 1$.

⁶In practice, one needs to know only the first half of these amplitudes, since degree- $(4n-8)$ amplitudes are anti-analytic (formerly known as googly $\overline{\text{MHV}}$ and they are simply given by degree-8* amplitudes, similarly degree- $(4n-12)$ are given by degree-12*, etc.

of the external lines in Figure 6 is also consistent with our conventions. The right vertex has n_1 lines, and the left one has n_2 lines in total, such that resulting amplitude A_n has $n = n_1 + n_2 - 2$ external lines. Suppressing summations over the distribution of n_1 and n_2 between the two vertices, we can write down an expression for the corresponding amplitude which follows immediately from (5.1) and Figure 6:

$$A_n = \frac{1}{\prod_{l=1}^n \langle l \ l + 1 \rangle} \frac{1}{q_I^2} \frac{\langle j \ j + 1 \rangle \langle i \ i + 1 \rangle}{\langle j \ \bar{I} \rangle \langle \bar{I} \ i + 1 \rangle \langle i \ I \rangle \langle I \ j + 1 \rangle} \times \int \prod_{A=1}^4 d\eta_I^A \delta^{(8)} \left(\lambda_{\bar{I}a} \eta_I^A + \sum_{l_2 \neq \bar{I}}^{n_2} \lambda_{l_2 a} \eta_{l_2}^A \right) \delta^{(8)} \left(\lambda_{Ia} \eta_I^A + \sum_{l_1 \neq I}^{n_1} \lambda_{l_1 a} \eta_{l_1}^A \right). \quad (5.6)$$

The two delta-functions in (5.6) come from the two vertices (5.1). The summations in the delta-functions arguments run over the $n_1 - 1$ external lines for right vertex, and $n_2 - 1$ external lines for the left one. The integration over $d^4 \eta_I$ arises in (5.6) for the following reason. Two separate (unconnected) vertices in Figure 6 would have $n_1 + n_2$ lines and, hence, $n_1 + n_2$ different η 's (and λ 's). However the I and the \bar{I} lines are connected by the propagator, and there must be only $n = n_1 + n_2 - 2$ η -variables left. This is achieved in (5.6) by setting

$$\eta_{\bar{I}}^A = \eta_I^A, \quad (5.7)$$

and integrating over $d^4 \eta_I$. The off-shell continuation of the internal spinors is defined as before,

$$\lambda_{Ia} = \sum_{l_1 \neq I}^{n_1} p_{l_1 a \dot{a}} \xi_{\text{Ref}}^{\dot{a}} = -\lambda_{\bar{I}a}. \quad (5.8)$$

We now integrate out four η_I 's which is made simple by rearranging the arguments of the delta-functions via $\int \delta(f_2) \delta(f_1) = \int \delta(f_1 + f_2) \delta(f_1)$, and noticing that the sum of two arguments, $f_1 + f_2$, does not depend on η_I .

The final result is

$$A_n = \frac{1}{\prod_{l=1}^n \langle l \ l + 1 \rangle} \delta^{(8)} \left(\sum_{i=1}^n \lambda_{ia} \eta_i^A \right) \prod_{A=1}^4 \left(\sum_{l_1 \neq I}^{n_1} \langle I \ l_1 \rangle \eta_{l_1}^A \right) \frac{1}{D}, \quad (5.9)$$

and D is the same as (3.7) used in sections 3 and 4,

$$\frac{1}{D} = \frac{1}{q_I^2} \frac{\langle j \ j + 1 \rangle \langle i \ i + 1 \rangle}{\langle j \ I \rangle \langle I \ i + 1 \rangle \langle i \ I \rangle \langle I \ j + 1 \rangle}. \quad (5.10)$$

There are 12 η 's in the superamplitude (5.9), and the coefficients of the Taylor expansion in η 's give all the component amplitudes of degree-12.

6. Conclusions

In this paper we have shown how all non-MHV tree-level amplitudes in $0 \leq \mathcal{N} \leq 4$ gauge theories can be obtained directly from the known MHV amplitudes using the scalar graph approach of Cachazo, Svrcek and Witten. As a specific example, we have focussed on amplitudes which are next-to-MHV, i.e. contain three negative helicity particles and an arbitrary number of positive helicity particles. By starting with amplitudes containing fermions, the reference spinor for the negative helicity gluons can be chosen to be that of the negative helicity fermion. As a consequence, the amplitudes are free of unphysical singularities for generic phase space points and no further helicity-spinor algebra is required to convert the results into a numerically usable form. The gluons only amplitudes can then be simply obtained as sums of fermionic amplitudes using the supersymmetric Ward identity. These amplitudes are therefore also immediately free of unphysical poles. We have provided expressions for $(-, -, -)$ amplitudes with a two and four fermions and shown how to construct the amplitudes for six fermions. The extension to amplitudes with four or more negative helicity particles is straightforward. In principle one could use the results presented here to write a numerical program for evaluating generic processes involving fermions and bosons [24, 25].

All of these results can be recovered from Nair's $\mathcal{N} = 4$ supervertex. This analytic vertex generates all possible interactions that depend only on products of $\langle \lambda_i \lambda_j \rangle$. Interestingly, all of the allowed vertices are not MHV. For example, $A_n(g^-, \Lambda^{1+}, \Lambda^{2+}, \Lambda^{3+}, \Lambda^{4+})$. This implies that the scalar graph approach is not primarily based on MHV amplitudes.

The next logical step is to extend the formalism to the computation of loop graphs. The twistor space approach of Ref. [2] may once again shed light on the structure of gauge theory amplitudes at the loop level [7]. Also, the simplified (four-dimensional) helicity amplitudes for arbitrary numbers of legs presented here may provide new impetus to computing loop amplitudes in supersymmetric theories using the unitarity approach [26] for sewing tree amplitudes to form loops.

Acknowledgements

We thank Arnd Brandenburg, Lance Dixon and Gabriele Travaglini for illuminating discussions. GG is supported by a grant from the State Scholarship Foundation of Greece (I.K.Y.). EWNG and VVK acknowledge PPARC Senior Fellowships. This work was supported in part by the EU Fifth Framework Programme 'Improving Human Potential', Research Training Network 'Particle Physics Phenomenology at High Energy Colliders', contract HPRN-CT-2000-00149.

References

- [1] F. Cachazo, P. Svrcek and E. Witten, “MHV vertices and tree amplitudes in gauge theory,” hep-th/0403047.
- [2] E. Witten, “Perturbative gauge theory as a string theory in twistor space,” hep-th/0312171.
- [3] G. Georgiou and V. V. Khoze, “Tree amplitudes in gauge theory as scalar MHV diagrams,” JHEP **0405** (2004) 070, hep-th/0404072.
- [4] C. J. Zhu, “The googly amplitudes in gauge theory,” JHEP **0404** (2004) 032 hep-th/0403115; J. B. Wu and C. J. Zhu, “MHV vertices and scattering amplitudes in gauge theory,” hep-th/0406085.
- [5] I. Bena, Z. Bern and D. A. Kosower, “Twistor-space recursive formulation of gauge theory amplitudes,” hep-th/0406133.
- [6] D. A. Kosower, “Next-to-maximal helicity violating amplitudes in gauge theory,” hep-th/0406175.
- [7] F. Cachazo, P. Svrcek and E. Witten, “Twistor space structure of one-loop amplitudes in gauge theory,” hep-th/0406177.
- [8] N. Berkovits, “An alternative string theory in twistor space for $N = 4$ super-Yang-Mills,” hep-th/0402045.
N. Berkovits and L. Motl, “Cubic twistorial string field theory,” JHEP **0404** (2004) 056 hep-th/0403187.
- [9] R. Roiban, M. Spradlin and A. Volovich, “A googly amplitude from the B-model in twistor space,” JHEP **0404** (2004) 012 hep-th/0402016;
R. Roiban, M. Spradlin and A. Volovich, “On the tree-level S-matrix of Yang-Mills theory,” hep-th/0403190.
- [10] A. Neitzke and C. Vafa, “ $N = 2$ strings and the twistorial Calabi-Yau,” hep-th/0402128.
N. Nekrasov, H. Ooguri and C. Vafa, “S-duality and topological strings,” hep-th/0403167.
- [11] E. Witten, “Parity invariance for strings in twistor space,” hep-th/0403199.
- [12] S. Gukov, L. Motl and A. Neitzke, “Equivalence of twistor prescriptions for super Yang-Mills,” hep-th/0404085.
- [13] W. Siegel, “Untwisting the twistor superstring,” hep-th/0404255.
- [14] S. Giombi, R. Ricci, D. Robles-Llana and D. Trancanelli, “A note on twistor gravity amplitudes,” hep-th/0405086.
- [15] A. D. Popov and C. Saemann, “On supertwistors, the Penrose-Ward transform and $N = 4$ super Yang-Mills theory,” hep-th/0405123.
- [16] N. Berkovits and E. Witten, “Conformal supergravity in twistor-string theory,” hep-th/0406051.

- [17] V. P. Nair, “A Current Algebra For Some Gauge Theory Amplitudes,” *Phys. Lett. B* **214** (1988) 215.
- [18] M. T. Grisaru, H. N. Pendleton and P. van Nieuwenhuizen, “Supergravity And The S Matrix,” *Phys. Rev. D* **15** (1977) 996;
M. T. Grisaru and H. N. Pendleton, “Some Properties Of Scattering Amplitudes In Supersymmetric Theories,” *Nucl. Phys. B* **124** (1977) 81.
- [19] S. J. Parke and T. R. Taylor, “An Amplitude For N Gluon Scattering,” *Phys. Rev. Lett.* **56** (1986) 2459.
- [20] F. A. Berends and W. T. Giele, “Recursive Calculations For Processes With N Gluons,” *Nucl. Phys. B* **306** (1988) 759.
- [21] F. A. Berends, R. Kleiss, P. De Causmaecker, R. Gastmans and T. T. Wu, *Phys. Lett. B* **103** (1981) 124;
P. De Causmaecker, R. Gastmans, W. Troost and T. T. Wu, *Nucl. Phys. B* **206** (1982) 53;
R. Kleiss and W. J. Stirling, *Nucl. Phys. B* **262** (1985) 235;
J. F. Gunion and Z. Kunszt, *Phys. Lett. B* **161** (1985) 333.
- [22] M. L. Mangano and S. J. Parke, “Multiparton Amplitudes In Gauge Theories,” *Phys. Rept.* **200** (1991) 301.
- [23] L. J. Dixon, “Calculating scattering amplitudes efficiently,” hep-ph/9601359.
- [24] F. A. Berends, W. T. Giele and H. Kuijf, *Phys. Lett. B* **232**, 266 (1989);
F. A. Berends, H. Kuijf, B. Tausk and W. T. Giele, *Nucl. Phys. B* **357**, 32 (1991);
F. Caravaglios and M. Moretti, *Phys. Lett. B* **358**, 332 (1995) hep-ph/9507237;
P. Draggiotis, R. H. Kleiss and C. G. Papadopoulos, *Phys. Lett. B* **439**, 157 (1998) hep-ph/9807207;
P. D. Draggiotis, R. H. Kleiss and C. G. Papadopoulos, *Eur. Phys. J. C* **24**, 447 (2002) hep-ph/0202201;
M. L. Mangano, M. Moretti, F. Piccinini, R. Pittau and A. D. Polosa, *JHEP* **0307**, 001 (2003) hep-ph/0206293.
- [25] T. Stelzer and W. F. Long, *Comput. Phys. Commun.* **81**, 357 (1994) hep-ph/9401258;
A. Pukhov *et al.*, hep-ph/9908288;
F. Yuasa *et al.*, *Prog. Theor. Phys. Suppl.* **138**, 18 (2000) hep-ph/0007053;
F. Krauss, R. Kuhn and G. Soff, *JHEP* **0202**, 044 (2002) hep-ph/0109036;
F. Maltoni and T. Stelzer, *JHEP* **0302** (2003) 027 hep-ph/0208156.
- [26] Z. Bern, L. J. Dixon, D. C. Dunbar and D. A. Kosower, “Fusing gauge theory tree amplitudes into loop amplitudes,” *Nucl. Phys. B* **435**:59 (1995) hep-ph/9409265;
Z. Bern, L. J. Dixon and D. A. Kosower, “Unitarity-based techniques for one-loop calculations in QCD,” *Nucl. Phys. Proc. Suppl.* **51C**:243 (1996) hep-ph/9606378.